Structural and Electronic Properties of Hetero-Transition-Metal Keggin Anions: A DFT Study of α/β-$[XW_{12}O_{40}]^{n-}$ (X = Cr^{VI}, V^{V}, Ti^{IV}, Fe^{III}, Co^{III}, Ni^{III}, Co^{II}, and Zn^{II}) Relative Stability

Fu-Qiang Zhang,[†,‡,*] Xian-Ming Zhang,[‡] Hai-Shun Wu,[‡,*] and Haijun Jiao[†]

The State Key Laboratory of Coal Conversion, Institute of Coal Chemistry, Chinese Academy of Sciences, Taiyuan, P. R. China, and School of Chemistry and Material Science, Shanxi Normal University, Linfen, P. R. China

Received: July 25, 2006; In Final Form: September 20, 2006

Density functional theory calculations have been carried out to investigate the electronic structures and the α/β relative stability of Keggin-typed $[XW_{12}O_{40}]^{n-}$ anions with transition metal as heteroatom X (X = Cr^{VI}, V^{V}, Ti^{IV}, Fe^{III}, Co^{III}, Ni^{III}, Co^{II} and Zn^{II}). Nice agreement in geometries between computation and experiment has been obtained, and the higher stability of the α isomer over the β one has been confirmed. Structural parameter analysis reveals that the $\{M_3O_{13}\}$ triads in both α and β isomers contract considerably with the increase of the negative anionic charge, while the overall size of both isomers shrinks only slightly. Fragment molecular orbital analysis shows that except α/β-$[TiW_{12}O_{40}]^{4-}$, the electronic structures of Keggin anions can be described by the insertion of the e and/or t_2 orbital of XO_4^{n-} into the frontier orbitals of $W_{12}O_{36}$ cage, and this leads to the specific redox property, which is different from that of the Keggin anions with main-group elements as heteroatoms. Energy decomposition analysis shows that the enhanced intrinsic stability of the α isomer in T_d arrangement of $W_{12}O_{36}$ shell and the larger deformation of the α over the β isomer are two dominating factors and contribute oppositely to the α/β relative stability.

Introduction

Keggin anions, $[XM_{12}O_{40}]^{n-}$ (M = Mo, W; heteroatom X = P^{V}, Si^{IV}, Ge^{IV}, Fe^{III}, Co^{II}, etc.), assembled by four $\{M_3O_{13}\}$ groups at the corners of a tetrahedron XO_4, comprise a large group of molecules in shape and composition in the polyoxometalate (POM) family.[1] Among the five cap-rotated isomers,[2] two more stable Keggin anions have been widely reported. The α isomer in T_d symmetry was synthesized first by Berzelius[3] and solved by Keggin;[4] and the β isomer in C_{3v} symmetry was observed first by Marignac[5] and determined by Yamamura and Sasaki.[6] As shown in Figure 1, the β isomer can be derived by 60° rotation of one of the M_3O_{13} triad around a 3-fold axis from the α isomer.[7] It should be noted that most structurally characterized Keggin anions are based on main-group heteroatom (MGX-Keggin), and those based on transition metals as heteroatom (TMX-Keggin) are only known for few α structures, and no β TMX-Keggin structures have been characterized by X-ray crystallography to date.[8]

Keggin anions can undergo multiple electron-reduction process with only slight structure distortion.[9] The special stability and the unique redox property of Keggin anions are the major reasons for making them attractive for application in catalysis and other technologies.[1b,c] For MGX-Keggin, the extra electrons unexceptionally fill into the delocalized LUMOs over the outer $M_{12}O_{36}$ sphere, and this yields the "blue" species.[10] However, for TMX-Keggin, the reduced electrons also can locate at the interior XO_4 subunit to yield the nonblue species. As a result, the redox property of TMX-Keggin can be substantially different from those of MGX-Keggin. For instance, α-$[V^{V}W_{12}O_{40}]^{3-}$ is a stronger oxidizing agent than α-$[PW_{12}O_{40}]^{3-}$ [11] and in particular, α-$[Co^{III}W_{12}O_{40}]^{5-}$ has been referred to as a "soluble anode" due to its very strong oxidizing power.[12]

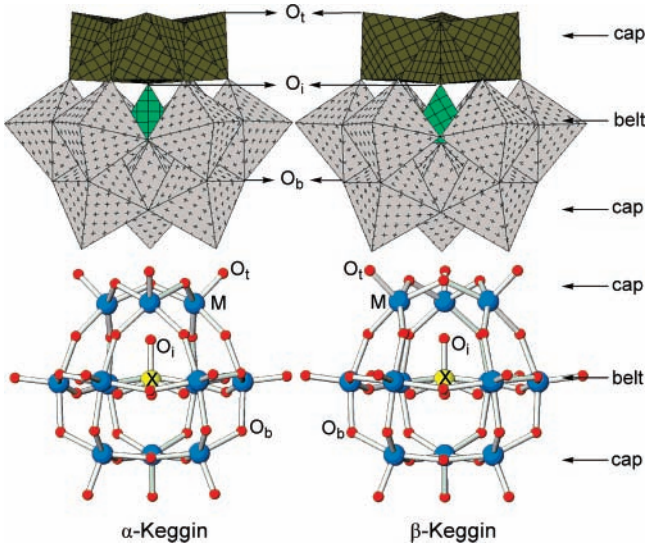

Figure 1. Polyhedral and ball-and-stick representations of α- and β-Keggin anions. Three types of oxygen atoms are given: terminal (O_t), interior (O_i), and bridging (O_b). The hatched $\{W_3O_{13}\}$ triad of β isomer has been rotated 60° about a 3-fold axis of α isomer.

Thanks to the rapid development of density functional theory (DFT) method and computer technology, high-level calculations on large metal systems such as POMs have been carried out recently.[13] As the most representative POMs, Keggin anions have been the major subject for theoretical investigations including relative stability,[14,15] electronic structure,[16] spectra,[17]

* Authors to whom correspondence should be addressed. E-mail: (F.-Q.Z.) zfq@dns.sxnu.edu.cn; (H.-S.W.) wuhs@dns.sxnu.edu.cn.
† Chinese Academy of Sciences.
‡ Shanxi Normal University.

10.1021/jp064732a CCC: $37.00
Published on Web 12/14/2006

TABLE 1: Selected Distances and Bond Lengths (in Ångstroms) for a Series of Keggin Anions[a]

X[b]	type	W−O$_b$[c]	W−O$_t$	X−O$_i$	W−O$_i$	W−X	sum[d]	W−W[e]	H−L[f]	ref[g]
Cr^{VI}	α	1.908−1.918	1.692	1.637	2.400	3.582	4.037	3.449−3.714	1.21	
	β	1.904−1.917	1.689	1.639	2.399	3.588	4.038	3.386−3.779	1.20	
V^{V}	α	1.911−1.919	1.699	1.694	2.341	3.560	4.035	3.401−3.715	2.61	
	expt[h]	1.843−1.990	1.69	1.68	2.34	3.55	4.02	3.37−3.72		31
	β	1.907−1.921	1.700	1.698	2.340	3.565	4.038	3.345−3.774	2.55	
Ti^{IV}	α	1.914−1.924	1.710	1.784	2.261	3.536	4.045	3.342−3.724	2.92	
	β	1.910−1.928	1.710	1.789	2.262	3.545	4.051	3.302−3.779	2.75	
Fe^{III}	α	1.914−1.933	1.723	1.834	2.208	3.512	4.042	3.299−3.719	2.15	
	expt	1.88−1.96	1.70	1.824	2.23	3.52	4.05	3.31−3.73		35
	β	1.910−1.935	1.721	1.838	2.210	3.522	4.048	3.266−3.767	1.99	
Co^{III}	α	1.911−1.937	1.723	1.823	2.214	3.510	4.037	3.300−3.714	0.69	
	expt	1.85−1.97	1.71	1.79	2.24	3.51	4.03	3.31−3.72		36
	β	1.909−1.936	1.721	1.828	2.215	3.519	4.043	3.268−3.760	0.51	
Ni^{III}	α	1.911−1.931	1.723	1.817	2.216	3.509	4.033	3.302−3.710	0.25	
	β	1.907−1.932	1.722	1.822	2.218	3.519	4.040	3.271−3.755	0.19	
Co^{II}	α	1.916−1.941	1.733	1.888	2.158	3.494	4.046	3.260−3.721	1.10	
	expt	1.89−1.99	1.71	1.895	2.16	3.49	4.05	3.27−3.71		38
	β	1.912−1.942	1.731	1.894	2.159	3.504	4.053	3.231−3.768	0.90	
Zn^{II}	α	1.916−1.941	1.733	1.895	2.155	3.495	4.050	3.259−3.722	2.90	
	expt	1.861−2.002	1.71	1.88	2.17	3.50	4.05	3.28−3.72		39
	β	1.913−1.953	1.731	1.905	2.156	3.505	4.059	3.229−3.769	2.71	

[a] Averaged values of X−O$_i$, W−O$_i$, W−O$_t$, W−X, and X−O$_t$ for β isomers are given. [b] Sextet, quintet, and quartet states for X = Fe^{III}, Co^{III}, and Co^{II}/Ni^{III}, respectively. [c] Observed intervals. [d] Sum of X−O$_i$ and W−O$_i$ bond lengths. [e] Two kinds W−W distances in the belt region are given. [f] Energy gap (eV) between LUMO and HOMO. [g] References. [h] X-ray data and averaged values are given.

redox property,[18] magnetic property,[19,20] metal−metal coupling,[21] acidity,[22,23] reactivity behavior,[24,25] and decomposition.[26] However, most studies were conducted on MGX-Keggin. Apart from the early extended-Hückel theory calculations,[27] DFT calculations were only performed on α-$[XW_{12}O_{40}]^{n-}$ (X = Fe^{III}, Co^{III}, and Co^{II}).[17f,19] Noting the absence of systematically high-level theoretical studies on the electronic structures and the α/β relative stabilities of TMX-Keggin, we carry out DFT calculations on α/β-$[XW_{12}O_{40}]^{n-}$ with X = Cr^{VI}, V^{V}, Ti^{IV}, Fe^{III}, Co^{III}, Ni^{III}, Co^{II}, and Zn^{II}. It is found that the redox property of these TMX-Keggin differs from each other, arising from the difference in their frontier orbitals.

Computational Details

All calculations were performed at the DFT level with DMol^3 program[28] in the Materials Studio of Accelrys Inc. The exchange and correlation energies were calculated using the Perdew and Wang functional[29] within the generalized gradient corrected approximation (GGA-PW91). The double numerical basis set augmented with *d*-polarization function was utilized, and ionic cores of metals were described by full electronic Darwin and mass-velocity relativistic effects (VPSR).[30] For the numerical integration, the *fine* quality mesh size was used and the real space cutoff of atomic orbital was set at 5.5 Å. The convergence criteria for structure optimization and energy calculation were set to FINE with the tolerance of density convergence in SCF, energy, gradient, and displacement of 1×10^{-6} e/Å,^{3} 2×10^{-5} au, 4×10^{-4} Å, and 5×10^{-4} Å, respectively. Spin restricted and unrestricted calculations were used for the close and open shell anions, respectively. The short-hand notation for Keggin anion without oxygen atoms, charge, and brackets is used, e.g., $Fe^{III}W_{12}$ for $[Fe^{III}W_{12}O_{40}]^{5-}$ and $Fe^{III}W_{12}1e$ for $[Fe^{III}W_{12}O_{40}]^{6-}$, where *e* specifics the number of the blue electrons.

Results and Discussion

Structure. All α- and β-XW_{12} anions were optimized under T_d and C_{3v} symmetry, respectively. In order to check the Jahn−Teller distortion, D_{2d} and C_s symmetry constraint was used for α- and β-$Co^{III}W_{12}$, respectively. The important parameters are provided in Table 1. In all structures, the calculated bond lengths within an average deviation of 0.02 Å agree well with the available experimental data. The largest deviation is only 0.03 Å for the W−W distance of α-$V^{V}W_{12}$,[31] and this validates the employed computational method nicely. However, it is very difficult to reproduce the X-ray structure of α-$Cu^{II}W_{12}$[32] with a discrepancy in Cu−O bond length of 0.08 Å, and therefore this anion is excluded from this study.

The sum of X−O$_i$ and W−O$_i$ bond lengths (O$_i$ is the interior oxygen atoms, Figure 1) is one of the important parameters for characterizing the size of the inner cavity of Keggin anions. In recent studies Weinstock et al.[33] have shown that the X−O$_i$ bond length changes with heteroatom X; however, the sum remains fairly constant, i.e., near to 4.00 Å (3.96, 4.01, 3.98, and 4.00 Å for α-PW_{12}, α-GaW_{12}, α/β-SiW_{12}, and α/β-AlW_{12}, respectively). As listed in Table 1, the sum of 4.035−4.059 Å in this work is subtly (∼0.05 Å) larger than 4.00 Å, reproducing well the general trend on one hand, and on the other hand revealing slight expansion of the inner cavity under the influence of enlarged size of XO_4. This similarity was thought to support the clathrate model,[34] which suggests that Keggin anion can be viewed as a XO_4 subunit encapsulated into the $M_{12}O_{36}$ cage. As shown in Figure 2, the N-shaped pattern of the sum is closely related to metal radius[35] of the central heteroatom X.

Similar to the sum, the distance of W addenda to central heteroatom (W−X) is another important parameter reflecting the size of the inner cavity. As listed in Table 1, W−X decreases from 3.582 to 3.494 Å for the α isomers and from 3.588 to 3.504 Å for the β isomers in the order of $Cr^{VI} > V^{V} > Ti^{IV} > Fe^{III} \sim Co^{III} \sim Ni^{III} > Co^{II} \sim Zn^{II}$. In contrast to the sum, W−X is almost independent of the X size but is closely related to the anionic charge (Figure 3). For example, for the −5 charged α anions, W−X is very close to 3.51 Å (3.512, 3.510, and 3.509 Å for X = Fe^{III}, Co^{III}, and Ni^{III}, respectively, from calculation; and 3.51 Å[36,37] for X = Fe^{III} and Co^{III} from experiment). Interestingly, the experimental W−X distances of the −5 charged α-AlW_{12} and α-GaW_{12} are almost the same.[33] For −6 charged α anions, the W−X is close to 3.50 Å (3.494 and 3.495 Å from calculation vs 3.50[38] and 3.49 Å[39] for X = Co^{II} and Zn^{II} from experiment, respectively). Similar results also are observed in the β isomers. It is noteworthy that due to the

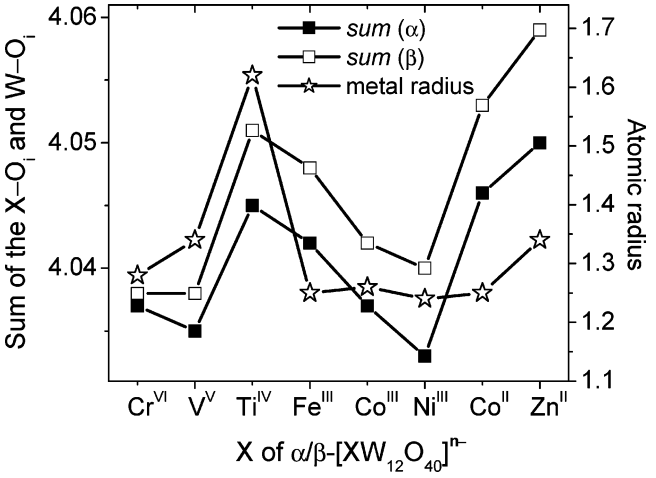

Figure 2. Sum of the W−O$_i$ and X−O$_i$ bond lengths (Å) along with X for α/*β*-[XW$_{12}$O$_{40}$]$^{n-}$.

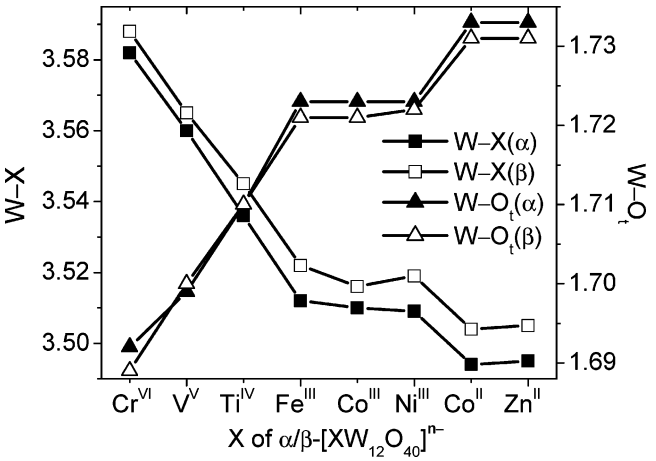

Figure 3. Bond lengths of W−X and W−O$_t$ (Å) along with X for α/*β*-[XW$_{12}$O$_{40}$]$^{n-}$.

general spherical shape of Keggin anions W−X can be viewed as the radius of their inner cavity. As a result, the variation of W−X can reflect the subtle change of the Keggin structure. For example, the decrease of W−X signifies that the cavity is shrunk up to 0.1 Å with the increase of the anionic charge from −2 to −6. Moreover, bond lengths of W to terminal oxygen atom (W−O$_t$) also relate closely to the charges of the Keggin anions but exhibit an increasing trend (Figure 3).

There are two types of M−M distance in α and *β* structures, i.e., the short one inside the {M$_3$O$_{13}$} triad (*intratriad*) and the long one between the neighboring {M$_3$O$_{13}$} triads (*intertriad*). The main difference between α and *β* structures lies in the equatorial M$_6$O$_6$ belt (Figure 1),[40] and the parameters in the belt region deserve great interests. As shown in Figure 4, the intratriad W−W distances (W−W$_{intra}$) decreases linearly with the increase of the negative charge for both isomers.[41] Importantly, the shrinkage of W−W$_{intra}$ reaches 0.16 Å as the charge goes from −2 to −6, revealing considerable contraction of the M$_6$O$_6$ belt. Differently, the intertriad W−W distances (W−W$_{inter}$) relate with the size of X and only vary slightly (0.01−0.03 Å). The variation in W−W is always accompanied by the change of the W−O−W bond angles, e.g., the intratriad W−O−W angle (W−O−W$_{intra}$) decreases about 14° in α isomers and 12° in *β* isomers, while the intertriad W−O−W angle (W−O−W$_{inter}$) varies only about 3° in both isomers. Indeed, the change of W−W and W−O−W in the belt region is also found in the other parts of the structures.[42]

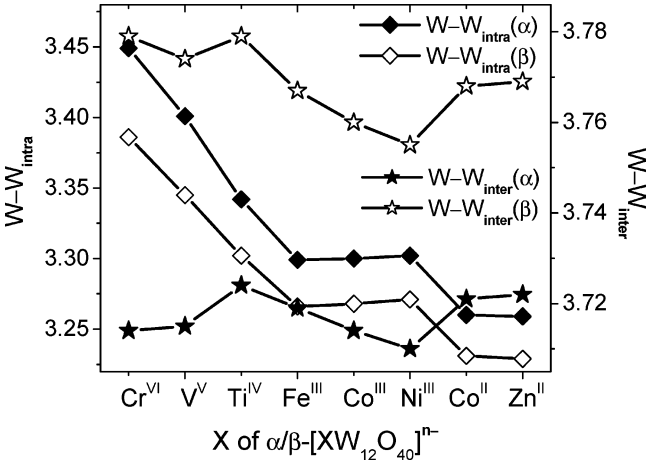

Figure 4. Distances of W−W$_{intra}$ and W−W$_{intra}$ (Å) in the belt region along with X for α/*β*-[XW$_{12}$O$_{40}$]$^{n-}$.

To summarize, the parameters of Keggin structures can be generally divided into two sets: the first set (W−X, W−O$_t$, W−W$_{intra}$, W−O−W$_{intra}$) is closely related to the charge, while the second set (sum, W−W$_{inter}$, W−O−W$_{inter}$) is intimately related to the size of X. As indicated by the variations of W−W$_{intra}$ and W−O−W$_{intra}$, the increase of the charge can induce significant contraction of the {M$_3$O$_{13}$} triads in both α and *β* isomers. However, both W−X and sum vary in a small range (∼0.1 Å), exhibiting that the overall size of Keggin anions varies only slightly with different X or charge.

Electronic Structure. The fully oxidized Keggin anion can be viewed as the W$_{12}$O$_{36}$ cage encapsulating one charged XO$_4^{n-}$ subunit. In the absence of the XO$_4^{n-}$, the empty W$_{12}$O$_{36}$ cage has a simple electronic structure composed by two well-separated sets of molecular energy levels with a HOMO−LUMO (H − L) gap of 2.80 and 3.01 eV for α and *β* structures, respectively. The low-lying delocalizing orbitals over the oxygen atoms comprise a predominantly Op nonbonding band (e.g., 35a$_1$, 84t$_2$, 63t$_1$ and 49e in Figure 5). Two types of orbitals are observed in the high-lying set. The first type represents weak *π*-antibonding interactions between the symmetry-adapted metal d$_{xy}$-liked and the bridging-oxygen p orbitals, delocalizing largely over the d-shells of the tungsten atoms (e.g., 50e and 64t$_1$ in Figure 5). The second type corresponds to d orbitals of the W$_3$O$_{13}$ triad fragments (e.g., 36a$_1$ in Figure 5). As X being transition metal, the general configuration XO$_4^{n-}$ is 1t$_1$2e7t$_2$-7a$_1$ and 8e1a$_2$9e10e13a$_1$14a$_1$ under T_d and C_{3v} symmetry, respectively. On the basis of group theory, there is a simply respective relationship between the two groups of orbitals (1t$_1$ ↔ 8e + 1a$_2$, 2e ↔ 9e, 7t$_2$ ↔ 10e + 13a$_1$, and 7a$_1$ ↔ 14a$_1$). The 2e and 7t$_2$ are more interesting for XO$_4^{n-}$/T_d, while 9e, 10e, and 13a$_1$ are more important for XO$_4^{n-}$/C_{3v}, because they are products of the low-energy d orbitals of X and the symmetry-adapted sp orbitals of four oxygen atoms. According to frontier orbital interacting types between XO$_4^{n-}$ and W$_{12}$O$_{36}$, Keggin anions in the paper can be divided into four sets.

The first set includes V^{V}W$_{12}$ and Cr^{VI}W$_{12}$ with X having closed-shell d^0. The qualitative fragment molecular orbital interaction diagram of α-V^{V}W$_{12}$ is shown in Figure 5. During the formation process of α-V^{V}W$_{12}$, the 2e (LUMO) of V^{V}O$_4^{3-}$/T_d directly inserts into the energy level between HOMO (49e^4) and LUMO (50e) of W$_{12}$O$_{36}$/T_d cage and becomes LUMO (51e) of the anion, while the frontier molecular orbitals (FMOs)

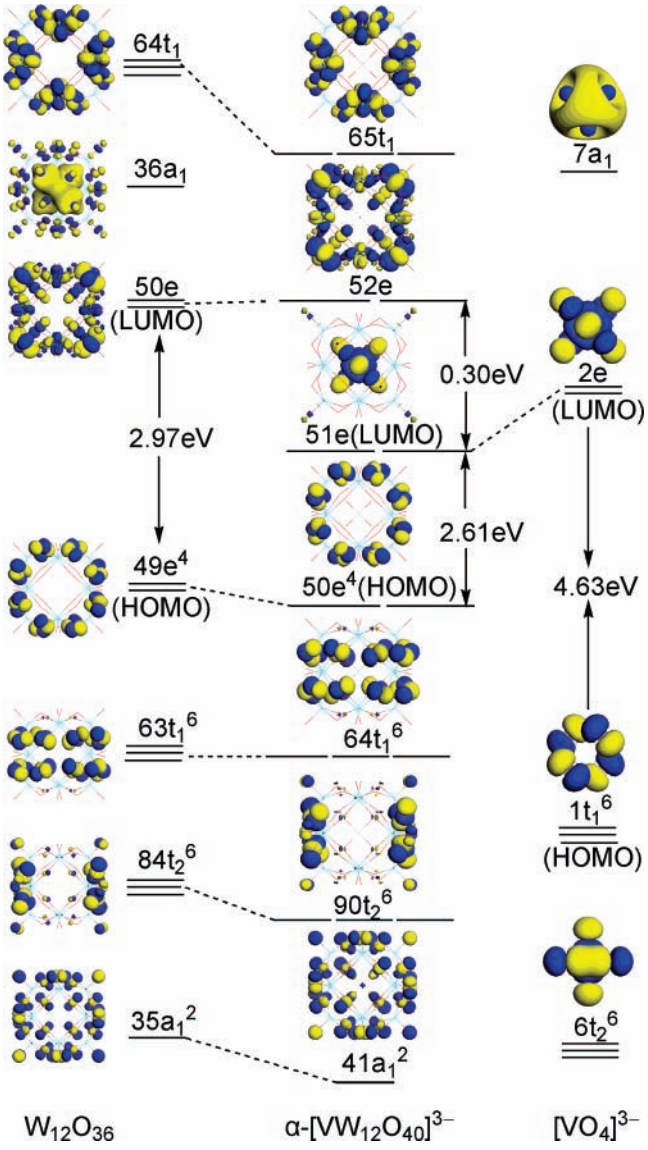

Figure 5. Qualitative molecular orbital diagram of α-$[V^{V}W_{12}O_{40}]^{3-}$ showing the contributions of the VO_4^{3-} and $W_{12}O_{36}$ fragments.

of $W_{12}O_{36}$ cage are transformed into the orbitals of the Keggin anions with slight energy relaxations. As a result, the H − L gap is lowered as compared to the parent $W_{12}O_{36}$ cage. It has been shown that there is a direct relationship between the energy of LUMO and oxidizing power of Keggin anions.[13a] Compared to the H − L gap of 2.91−2.97 eV (~2.8 eV[19]) of α-Keggin tungstates with main group X = P^{V}, Si^{IV}, and Al^{III}, the H−L gap of 2.61 eV in α-$V^{V}W_{12}$ is about 0.3−0.4 eV lower. The lower LUMO energy in α-$V^{V}W_{12}$ shows the higher reduction potential, as confirmed by the cyclic voltammetric experiment.[11] Moreover, from Figure 5 it is easy to see that one-electron reduction of α-$V^{V}W_{12}$ should take place at the $V^{V}O_4^{3-}$ subunit, in accordance with the recent experiment data.[11] This behavior differs significantly from α-Keggin anions with main group X[9,13a,14] in which the addenda metal ions of the $M_{12}O_{36}$ shell prefer to be reduced to yield blue species.

However, the LUMO of β-$V^{V}W_{12}$ comes from the 9e (LUMO) of the $V^{V}O_4^{3-}$ fragment while the other MOs are those slightly touched β-$W_{12}O_{36}/C_{3v}$ MOs (see Figure S3 in Supporting Information). Compared to the α isomer, further lowering of the H−L gap (2.55 eV) of β-$V^{V}W_{12}$ suggests the enhanced oxidizing power, in accordance with the fact that β isomer can be reduced at more positive potential than α isomer.[1,43a] Similar to the α counterpart, the first extra electron in β-$V^{V}W_{12}$ will localize at the $V^{V}O_4^{3-}$ subunit to yield nonblue species. Moreover, it is found that α- and β-$Cr^{VI}W_{12}$ have the similar molecular orbital interaction diagrams as α- and β-$V^{V}W_{12}$ and a lower H−L gap (1.20−1.21 eV).

The second set includes the α- and β-$Ti^{IV}W_{12}$ anions. Sharing the same electronic configuration with the isoelectronic XW_{12} (X = Cr^{VI} and V^{V}), $Ti^{IV}W_{12}$ behave quite differently. The main feature is that the FMOs of both α- and β-$Ti^{IV}W_{12}$ come almost from the $W_{12}O_{36}$ fragment (α isomer in Figure 6 and β isomer in Supporting Information), and the contribution from $Ti^{IV}O_4^{4-}$ is negligible. Therefore, the reduction of $Ti^{IV}W_{12}$ forms the blue species. In addition, the computed H−L gap for the α and β isomers is 2.92 and 2.75 eV, respectively, and they are larger than those of the isoelectronic XW_{12} (X = Cr^{VI} and V^{V}).

The third set includes the α- and β-$Zn^{II}W_{12}$ anions, in which the triply degenerate $7t_2^6$ (HOMO) of $Zn^{II}O_4^{6-}$ contributes mainly to their HOMO/HOMOs ($91t_2^6$ for α and $132a_1$/206e for β isomer), while their LUMO come from $W_{12}O_{36}$ (52e for α and 197e for β isomer). It is to note that the HOMOs of $Zn^{II}W_{12}$ anion ($91t_2$ and 51e for α isomer; $132a_1$, 206e, and 205e for β isomer) are almost degenerate within a difference of only 0.03−0.07 eV, and the computed H−L gap of α-$Zn^{II}W_{12}$ (2.90 eV) is very close to those of α-$Ti^{IV}W_{12}$ (2.92 eV) and α-XW_{12} (X = As, Ge, and Ga; 2.90−2.94 eV), and that of β-$Zn^{II}W_{12}$ (2.71 eV) is close to those of β-$Ti^{IV}W_{12}$ (2.75 eV) and β-XW_{12} (X = As, Ge, and Ga; 2.72−2.78 eV).

The fourth set includes $Fe^{III}W_{12}$, $Co^{III}W_{12}$, $Ni^{III}W_{12}$, and $Co^{II}W_{12}$ in which X has partially occupied d orbitals ($d^{5\sim7}$). One interesting point of all the open-shell anions is that the unpaired electrons dominantly localize on XO_4 subunit and only 0.17−0.23 *e* delocalize over the $W_{12}O_{36}$ shell (see Supporting Information). In agreement with experiment,[36,44] our calculations identify that the ground states of α-$Fe^{III}W_{12}$, α-$Co^{III}W_{12}$, and α-$Co^{II}W_{12}$ are sextet (e^2t^3), quintet (e^3t^3), and quadruplet (e^4t^3), respectively. In addition, slight Jahn−Teller distortion from T_d to D_{2d} is observed in α-$Co^{III}W_{12}$ with 2.56 kcal/mol and from D_{2d} to C_s in β-$Co^{III}W_{12}$ with 1.36 kcal/mol. Since this distortion has only small energetic impact, we will discuss their FMO properties in T_d and D_{2d} symmetry for comparison.

For the α isomers, the XO_4^{n-}/T_d subunit shows occupations of $(2e\uparrow)^2(7t_2\uparrow)^3(2e\downarrow)^0$, $(2e\uparrow)^2(7t_2\uparrow)^3(2e\downarrow)^1$, and $(2e\uparrow)^2(7t_2\uparrow)^3(2e\downarrow)^2$ for X = Fe^{III}, Co^{III}, and Co^{II}/Ni^{III} ($e^2t_2^3$, $e^3t_2^3$, and $e^4t_2^3$), respectively. In α-XW_{12}, both e and t_2 orbitals of XO_4^{n-} are embedded into the FMOs of $W_{12}O_{36}$ cage, and two points can be drawn from the analysis of fragmental orbital interaction: (*i*) The $91t_2\uparrow$(spin-up), 51e↓(spin-down), and $91t_2\downarrow$ of α-XW_{12} come from the $7t_2\uparrow$, 2e↓, and $7t_2\downarrow$ of XO_4, respectively, while 50e↑ is from 49e↑ of the $W_{12}O_{36}$ cage. (*ii*) For −5 charged α-$X^{III}W_{12}$ (X = Fe^{III}, Co^{III}, and Ni^{III}) anions, 50e↑ and 51e↑ are mixing products of the 2e↑ of XO_4 and the 49e↑ of $W_{12}O_{36}$, in which 51e↑ is dominated by 49e↑ while 50e↑ is in a large part of 2e↑. Differently, for −6 charged α-$Co^{II}W_{12}$ 50e↓ comes from 49e↓ of $W_{12}O_{36}$ while 51e↑ comes from the 2e↑ of $Co^{II}O_4^{6-}$, respectively.

The differences in the energy level of 51e↑, $91t_2\downarrow$, and 52e↑ in α-XW_{12} (X = Fe^{III}, $Co^{III/II}$, Ni^{III}) lead to their different redox properties. For example, it can be deduced from Figure 6 that for α-$Co^{III}W_{12}$ the first extra electron should fill into the half-occupied 51e↓ orbital to yield α-$Co^{II}W_{12}$. The very low-energy level of 51e↓ in α-$Co^{III}W_{12}$ (energy gap between 51e↓ and $91t_2\uparrow$ is only 0.69 eV) is in accordance with its very strong oxidizing power.[12] However, due to the high level of the vacant $91t_2\downarrow$ in

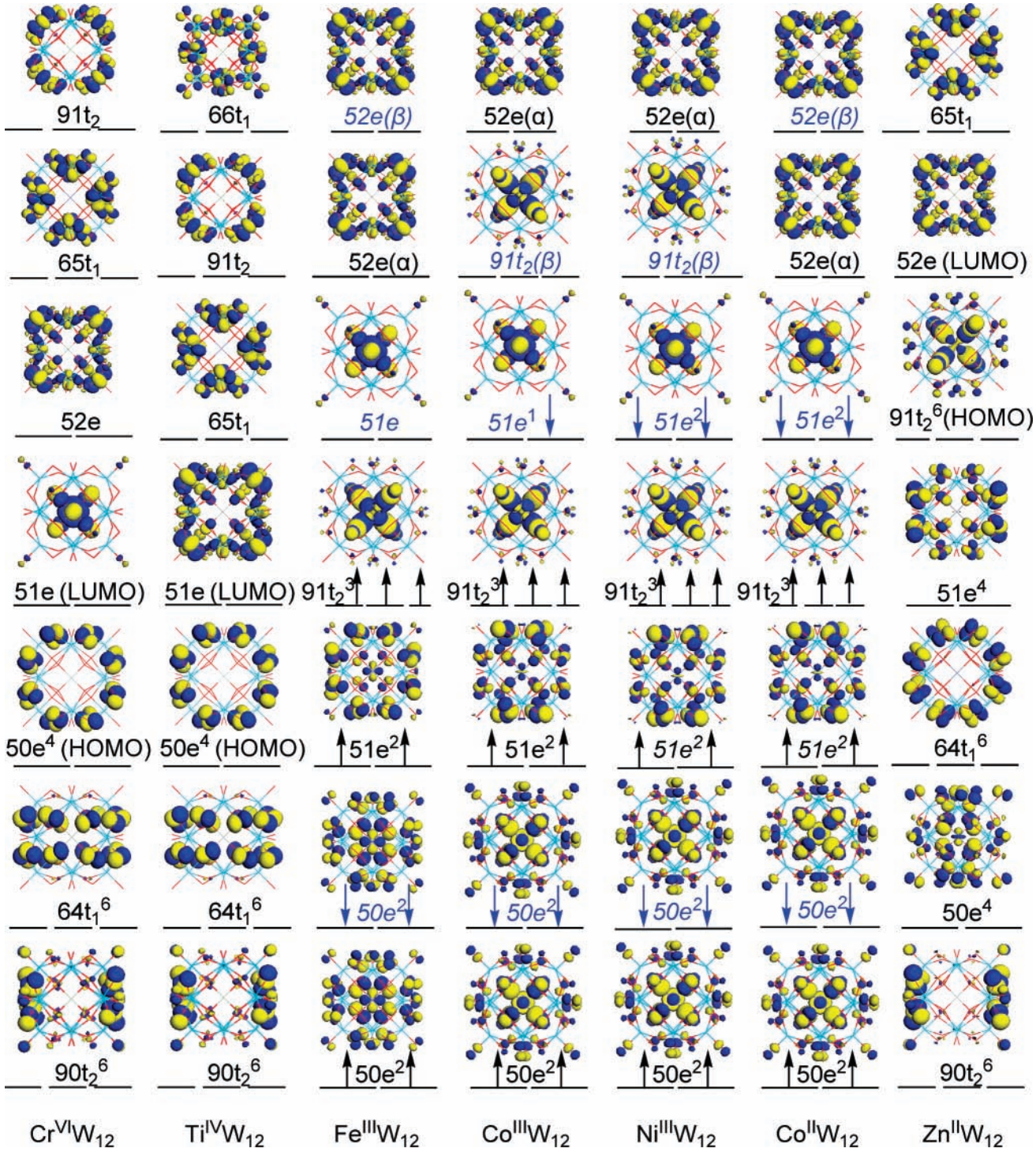

Figure 6. Spatial representation of the orbitals of α-$[XW_{12}O_{40}]^{n-}$ (X = Cr^{VI}, Ti^{IV}, Fe^{III}, Co^{III}, Ni^{III}, Co^{II}, and Zn^{II}). The "α" and "*β*" denote spin-up and spin-down orbitals, respectively.

α-$Co^{II}W_{12}$, subsequent reduction will take place on $W_{12}O_{36}$ and yield blue species α-$Co^{II}W_{12}$1e. This agrees with the well-known experimental evidence[44] and the theoretical studies.[17f,19] In contrast to the isoelectronic α-$Co^{II}W_{12}$, the LUMO of α-$Ni^{III}W_{12}$ comes from $7t_2\downarrow$ of $Ni^{III}O_4^{5-}$ subunit, and the one-electron reduction product of α-$Ni^{III}W_{12}$ should yield α-$Ni^{II}W_{12}$. For α-$Fe^{III}W_{12}$, however, it is very interesting to note that the reduction electron will delocalize over the α-$W_{12}O_{36}$ cage ($52e\uparrow$) to yield the blue species rather than locate at the $Fe^{III}O_4^{5-}$ subunit ($51e\downarrow$). This agrees with the experimental observation,[45] but in sharp contrast to our expectation since $51e\downarrow$ is lowered in energy. For this energetic disorder, Poblet and co-workers[19] suggested that this situation could be attributed to the special property of $51e\downarrow$, which is quite high in energy and slightly (0.19 eV) separated from the d-shells. As a result, the occupation of the first electron into 52e can be changed to energy favorable.

It is to note that the electronic properties of *β* anions in the fourth set mimic those of the corresponding α anions. For example, the 9e, 10e, and $13a_1$ orbitals ($9e^210e^213a_1^1$, $9e^310e^2$-$13a_1^1$, and $9e^410e^213a_1^1$ for X = Fe^{III}, Co^{III}, and Co^{II}/Ni^{III}, respectively) of XO_4^{n-}/C_{3v} are embedded into the FMOs of the $W_{12}O_{36}$ cage and become important parts of Keggin anions (See Figure S4 in Supporting Information). Based on this, it can be

TABLE 2: Three Kinds of Calculated Relative Energies (kcal/mol) Including Fragment Interaction Energy (ΔFIE), Deformation Energy (ΔDE), and Total Energy (ΔE_t) of the Keggin Anions Obtained by $\beta - \alpha$

X	ΔFIE	ΔDE	ΔE_t
Cr^{VI}	−1.45	−3.87	3.31
V^{V}	−1.99	−4.06	2.60
Ti^{IV}	−0.67	−7.17	0.80
Fe^{III}	4.88	−12.17	1.36
Co^{III}	3.95	−10.81	1.79
Ni^{III}	4.49	−10.61	2.54
Co^{II}	6.34	−12.39	2.60
Zn^{II}	6.33	−13.38	1.59

expected that the reduction products of the β isomers can mimic those of the α counterparts. Meanwhile, the H−L gaps of the β Keggin anions are generally lowered, as observed in the β MGX-Keggin anions.[14] For example, the H−L gap of β-$Co^{II}W_{12}$ and β-$Ni^{III}W_{12}$ are less than those of the corresponding α counterparts by about 0.20 and 0.10 eV (Table 1), respectively.

Relative Stability of α/β Isomers. Our calculations show the gradually decreased α/β relative stability (ΔE_t, Table 2) order of $Cr^{VI}O_4^{2-} > V^{V}O_4^{3-} \sim Co^{II}O_4^{6-} > Ni^{III}O_4^{5-} > Co^{III}O_4^{5-} > Zn^{II}O_4^{6-} > Fe^{III}O_4^{5-} > Ti^{IV}O_4^{4-}$, which differs significantly from that of MGX-Keggin. Both experimental[33] and theoretical studies[14] have evidenced that the α/β relative stability of MGX-Keggin XW_{12} (X = P^{V}, Si^{IV}, and Al^{III}) was closely related to anionic charge, e.g., in the decreased order of $PO_4^{3-} > SiO_4^{4-} > AlO_4^{5-}$. For TMX-Keggin, the α/$\beta$ relative stability order is complicated, and can be discussed on the basis of the electronic configuration of d^0, d^{5-7}, and d^{10} of X.

For TMX-Keggin with d^0 X, the α/β relative stability order is $Cr^{VI}O_4^{2-} > V^{V}O_4^{3-} > Ti^{IV}O_4^{4-}$. Similar to MGX-Keggin, the charge plays a critical role of influencing the α/β relative stability, i.e., the higher the anionic charge, the more stable the β isomer is. As a result, the largest stability in favor of α isomer is found for the least charged $Cr^{VI}W_{12}$ with ΔE_t of 3.31 kcal/mol, while the most stable β isomer corresponds to the highest negatively charged $Ti^{IV}W_{12}$ with ΔE_t of only 0.80 kcal/mol in this set.

For open-shell TMX-Keggin with d^{5-7} X, the order is $Co^{II}O_4^{6-} \sim Ni^{III}O_4^{5-} > Co^{III}O_4^{5-} > Fe^{III}O_4^{5-}$. In this set, the electronic configuration of X rather than anionic charge can affect the ΔE_t considerably. For example, $Fe^{III}W_{12}$, $Co^{III}W_{12}$, and $Ni^{III}W_{12}$ have the same negative charge, and the ΔE_t of the α/β isomers increases from $Fe^{III}W_{12}$ (d^5, 1.36 kcal/mol), $Co^{III}W_{12}$ (d^6, 1.79 kcal/mol), to $Ni^{III}W_{12}$ (d^7, 2.54 kcal/mol); while for the higher charged $Co^{II}W_{12}$ (d^7), the ΔE_t reaches 2.60 kcal/mol. However, $Zn^{II}W_{12}$ with d^{10} X, which is different from all the anions mentioned above (d^0 and d^{5-7}), has ΔE_t of 1.59 kcal/mol.

To get a better understanding of the factors influencing the α/β relative stability of TMX-Keggin, the following energy decomposition scheme is utilized.

$$W_{12}O_{36}\,(\text{free}) + XO_4^{n-}\,(\text{free}) = [XW_{12}O_{40}]^{n-} \qquad (1)$$

The β/α energy difference can be evaluated using

$$\Delta E_t = \Delta E_{free} + \Delta DE + \Delta FIE \qquad (2)$$

where FIE is the fragment interaction energy between $W_{12}O_{36}$ and XO_4^{n-}; DE is the sum of the deformation energies of $W_{12}O_{36}$ and XO_4^{n-} from their fully relaxed conformations; E_{free} is the sum of energies of the fully relaxed $W_{12}O_{36}$ and XO_4^{n-}; E_t is the energy of the optimized Keggin anion. The prefix "Δ" denotes the energy difference defined as (β − α) and the computed data are given in Table 2.

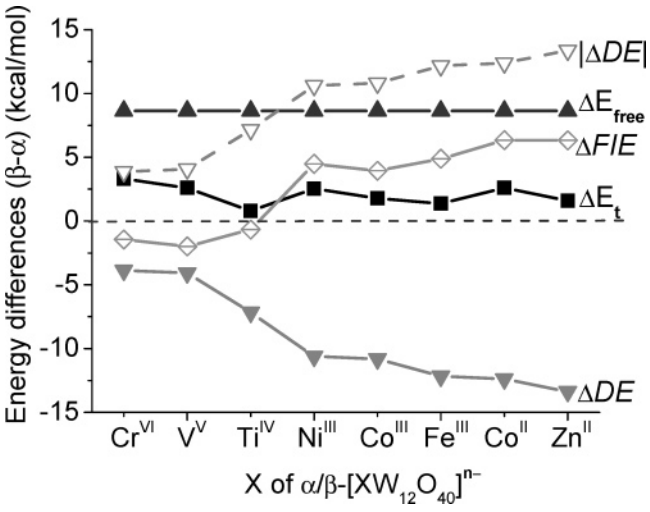

Figure 7. Five kinds of energy differences as functions of heteroatoms (X) for α/β-$[XW_{12}O_{40}]^{n-}$(X = Cr^{VI}, V^{V}, Ti^{IV}, Ni^{III}, Fe^{III}, Co^{III}, Co^{II}, and Zn^{II}). |ΔDE| is the absolute value of ΔDE.

It can be deduced from eq 2 that three principal factors affect the α/β relative stability (ΔE_t), namely, ΔE_{free}, ΔDE, and ΔFIE. ΔE_{free} is a positive constant (8.64 kcal/mol), exhibiting the intrinsic stability of the α cage over the β one of $W_{12}O_{36}$.[46] ΔDE is negative (−3.87 to −13.38 kcal/mol) and decreases with X in the order of $Cr^{VI} > V^{V} > Ti^{IV} > Co^{III} \sim Ni^{III} > Fe^{III} > Co^{II} > Zn^{II}$ (Table 2), reflecting that α isomer is stronger distorted than the β isomer as the anionic charge increases. The ΔFIE (−1.99 to 6.34 kcal/mol) increases in the order $Cr^{VI} \sim V^{V} < Ti^{IV} < Co^{III} < Ni^{III} \sim Fe^{III} < Co^{II} \sim Zn^{II}$, revealing that the host−guest interaction generally favors the α isomer as the anionic charge increases.

As listed in Table 2, for the less negatively charged (−2 to −4) XW_{12} anions with X = Cr^{VI}, V^{V}, and Ti^{IV}, the α/β relative stability is mainly controlled by two competing forces, i.e., ΔE_{free} (8.64 kcal/mol) and ΔDE (−3.87 to −7.17 kcal/mol), while ΔFIE (−0.67 to −1.99 kcal/mol) favors the β isomer only slightly. Interestingly, as the charge goes from −4 to −5, both ΔDE and ΔFIE exhibit a considerable increase in their absolute values (Figure 7). As a result, for the more negatively charged (−5 and −6) XW_{12} anions with X = Fe^{III}, $Co^{III/II}$, Ni^{III}, and Zn^{II}, ΔDE (−10.61 to −13.38 kcal/mol), ΔFIE (3.95 to 6.34 kcal/mol), and ΔE_{free} (8.64 kcal/mol) are important components of ΔE_t. Obviously, in all the cases ΔE_{free} and ΔDE are dominant while ΔFIE is subordinate, and the large deformation energy of the α isomer (ΔDE) is the sole factor responsible for the decrease of ΔE_t. This result is roughly in accordance with the recent study of Poblet et al.,[14a] and they also suggested that the stability of α MGX-Keggin isomer over the β one is coming from its organization in $W_{12}O_{36}$. Moreover, the opposite changing trends of ΔDE ($Cr^{VI} > V^{V} > Ti^{IV} > Co^{III} \sim Ni^{III} > Fe^{III} > Co^{II} > Zn^{II}$) and ΔFIE ($Cr^{VI} \sim V^{V} < Ti^{IV} < Co^{III} < Ni^{III} \sim Fe^{III} < Co^{II} \sim Zn^{II}$) reveal that negative charge of the cluster is one of the key origins influencing the α/β relative stability. Considering the constant of ΔE_{free} in eq 2, the complexity of ΔE_t in this paper can be attributed to the different changing magnitude of ΔFIE and ΔDE related to the electronic configuration of X.

Conclusions

High level DFT calculations have been performed on a series of Keggin anions α/β-$[XW_{12}O_{40}]^{n-}$ with transition metal het-

eratom (X = Cr^{VI}, V^{V}, Ti^{IV}, Fe^{III}, Co^{III}, Ni^{III}, Co^{II}, and Zn^{II}). The structural parameters from experiment have been nicely reproduced by computation, and the conventional trend of the higher stability of α over the β isomer has been confirmed. Furthermore, our calculations have the following results:

(*i*) The GGA-PW91/DND approach is adequate to describe the geometries, energies, and electronic structures of the Keggin anions with transition metal heteroatoms.

(*ii*) The important parameters of Keggin structures vary regularly with respect to the size of X or the anionic charge. Induced by anionic charge, considerable contraction is observed in the $\{M_3O_{13}\}$ triads for both α and β isomers.

(*iii*) The α/β-$[Ti^{IV}W_{12}O_{40}]^{4-}$ anions exhibit similar electronic structure to hetero-main-group-element Keggin anions while others with X = Cr^{VI}, V^{V}, Fe^{III}, Co^{III}, Ni^{III}, Co^{II}, and Zn^{II} show different properties due to the participation of the d orbitals of X. The β isomer is always expected to be more powerful oxidizing than α partner.

(iv) There are three factors governing the α/β relative stability. For the low-charge anions, the intrinsic stability of α arrangement in $W_{12}O_{36}$ is dominant; while for the high-charge anions, both the host−guest interaction and the structural deformation become important.

This work is helpful to get better understanding of electronic effects induced by different X, which is critical and fundamental in design and selection of appropriate polyoxometalate catalysts. The clarification of the difference between hetero-transition-metal and hetero-main-group-element Keggin tungstates may shed new insight into the basic properties of Keggin polyoxometalates.

Acknowledgment. This work is supported by the National Natural Science Foundation of China (20673070).

Supporting Information Available: Total electronic energies of Keggin anions, single-point energies of the isolated $W_{12}O_{36}$ and XO_4^{n-}, W−W distances of the β isomers, W−O−W angles of α and β isomers, the qualitative molecular orbital diagram of β-$[V^{V}W_{12}O_{40}]^{3-}$, and molecular orbitals of the β Keggin anions. This material is available free of charge via http://pubs.acs.org.

References and Notes

(1) (a) Pope, M. T. *Heteropoly and Isopoly Oxometalates*; Springer-Verlag: Berlin, 1983. (b) Hill, C. L., Ed. *Chem. Rev.* **1998**, *98*, 1−390. (Special issue on polyoxometalates). (c) Pope, M. T.; Müller, A. *Polyoxometalates: From Platonic Solids to Anti-retroviral Activity*; Kluwer: Dordrecht, The Netherlands, 1993. (d) Clemente-Juan, J. M.; Coronado, E. *Coord. Chem. Rev.* **1999**, *193*−*195*, 361−394.

(2) Baker, L. C. W.; Figgis, J. S. *J. Am. Chem. Soc.* **1970**, *92*, 3794.

(3) Berzelius, J. *Poggendorff's Ann. Phys.* **1826**, *6*, 369.

(4) Keggin, J. F. *Nature* **1933**, *131*, 908.

(5) Marignac, C. *Ann. Chim. Phys.* **1864**, *3*, 1.

(6) Yamamura, K.; Sasaki, Y. *J. Chem. Soc. Chem. Commun.* **1973**, 648.

(7) Chalmers, R. A.; Sinclair, A. G. *Anal. Chim. Acta* **1965**, *33*, 384.

(8) (a) Cambridge Crystallographic Data Center (CCDC), Cambridge, U.K. (b) Fiz-Karlsruhe, Karlsruhe, Germany (via STN International).

(9) Maestre, J. M.; Bo, C.; Poblet, J.-M.; Cansañ-Pastor, R.; Gomez-Romero, P. *Inorg. Chem.* **1998**, *37*, 3444.

(10) Steckhan, E.; Sadakane, M. *Chem. Rev.* **1998**, *98*, 219 and references therein.

(11) Himeno, S.; Takamoto, M.; Higuchi, A.; Maekawa, M. *Inorg. Chim. Acta* **2003**, *348*, 57.

(12) (a) Eberson, L.; Wistrand, L.-G. *Acta Chem. Scand. B* **1980**, *34*, 349. (b) Weinstock, I. A. *Chem. Rev.* **1998**, *98*, 113.

(13) (a) Poblet, J. M.; López, X.; Bo, C. *Chem. Soc. Rev.* **2003**, *32*, 297 and references therein. (b) Rohmer, M.-M.; Bénard, M.; Blaudeau, J.-P.; Maestre, J.-M.; Poblet, J.-M. *Coord. Chem. Rev.* **1998**, *178*−*180*, 1019 and references therein.

(14) (a) López, X.; Maestre, J. M.; Bo, C.; Poblet, J.-M. *J. Am. Chem. Soc.* **2001**, *123*, 9571. (b) López, X.; Poblet, J.-M. *Inorg. Chem.* **2004**, *43*, 6863.

(15) Guan, W.; Yan, L.; Su, Z.-M.; Liu, S.; Zhang, M.; Wang, X. *Inorg. Chem.* **2005**, *44*, 100.

(16) For example, please see: (a) Rohmer, M. M.; Bénard, M.; Cadot, E.; Sécheresse, F. In *PolyoxometalateChemistry: From Topology via Self-Assembly to Applications*; Pope, M. T., Müller, A., Eds.; Kluwer Academic Publishers: Dordrecht, 2001; pp 117. (b) Bridgeman, A. J.; Cavigliasso, G. *J. Phys. Chem. A* **2003**, *107*, 6613. (c) Duclusaud, H. D.; Borshch, S. A. *Inorg. Chem.* **1998**, *38*, 3489. (d) Suaud, N.; Gaita-Ariño, A.; Clemente-Juan, J. M.; Sánchez-Marin, J.; Coronado, E. *J. Am. Chem. Soc.* **2002**, *124*, 15134. (e) Kholdeeva, O. A.; Trubitsina, T. A.; Maksimovskaya, R. I.; Golovin, A. V.; Neiwert, W.; Kolesov, B. A.; López, X.; Poblet, J. M. *Inorg. Chem.* **2004**, *43*, 2284.

(17) (a) Bridgeman, A. J. *Chem. Eur. J.* **2004**, *10*, 2935. (b) Bridgeman, A. J. *J. Chem. Phys.* **2003**, *287*, 55. (c)Watras, M. J.; Teplyakov, A. V. *J. Phys. Chem. B* **2005**, *109*, 8928. (d) Guo, Y.-R.; Pan, Q.-J.; Wei, Y.-D.; Li, Z.-H.; Li, X. *J. Mol. Struct. (Theochem)* **2005**, *676*, 55. (e) Bagno, A.; Bonchio, M.; Sartorel, A.; Scorrano, G. *Chem. Phys. Chem.* **2003**, *4*, 517. (f) Maestre, J. M.; López, X.; Bo, C.; Poblet, J.-M. *Inorg. Chem.* **2002**, *41*, 1883. (g) Hashimoto, M.; Koyano, G.; Mizuno, N. *J. Phys. Chem. B* **2004**, *108*, 12368.

(18) (a) Duclusaud, H.; Borshch, S. A. *Inorg. Chem.* **1999**, *38*, 3489. (b) Zueva, E. M.; Chermette, H.; Borshch, S. A. *Inorg. Chem.* **2004**, *43*, 2834. (c) López, X.; Bo, C.; Poblet, J.-M. *J. Am. Chem. Soc.* **2002**, *124*, 12574.

(19) Maestre, J. M.; López, X.; Bo, C.; Poblet, J.-M.; Casan-Pastor, N. *J. Am. Chem. Soc.* **2001**, *123*, 3749.

(20) Wang, Y.; Zheng, G.; Morokuma, K.; Geletii, Y. V.; Hill, C. L.; Museav, D. G. *J. Phys. Chem. B* **200**6, *110*, 5230.

(21) Bagno, A.; Bonchio, M. *Angew. Chem., Int. Ed.* **200**5, *44*, 2023.

(22) Ganapathy, S.; Fournier, M.; Paul, J. F.; Delevoye, L.; Guelton, M.; Amoureux, J. P. *J. Am. Chem. Soc.* **2002**, *124*, 7821.

(23) (a) Bardin, B. B.; Bordawekar, S. V.; Neurock, M.; Davis, R. J. *J. Phys. Chem. B* **1998**, *102*, 10817. (b) Janik, M. J.; Davis, R. J.; Neurock, M. *J. Phys. Chem. B* **2004**, *108*, 12292. (c) Yang, J.; Janik, M. J.; Ma, D.; Zheng, A.; Zhang, M.; Neurock, M.; Davis, R. J.; Ye, C.; Deng, F. *J. Am. Chem. Soc.* **2005**, *127*, 18274. (d) Campbell, K. A.; Janik, M. J.; Davis, R.; Neurock, M. *Langmuir* **2005**, *21*, 4737. (e) Janik, M. J.; Davis, R. J.; Neurock, M. *J. Am. Chem. Soc.* **2005**, *127*, 5238.

(24) (a) de Visser, S. P.; Kumar, D.; Neumann, R.; Shaik, S. *Angew. Chem., Int. Ed.* **2004**, *43*, 5661. (b) Kumar, D.; Derat, E.; Khenkin, A. M.; Neumann, R.; Shaik, S. *J. Am. Chem. Soc.* **2005**, *127*, 17712.

(25) (a) Prabhakar, R.; Morokuma, K.; Hill, C. L.; Musaev, D. G. *Inorg. Chem.* **2006**, *45*, 5703. (b) Janik, M. J.; Davis, R. J.; Neurock, D. M. *Catal. Today* **2005**, *105*, 134. (c) Musaev, D. G.; Morokuma, K.; Geletii, Y. V.; Hill, C. L. *Inorg. Chem.* **2004**, *43*, 7702.

(26) Janik, M. J.; Bardin, B. B.; Davis, R.; Neurock, M. *J. Phys. Chem. B* **2006**, *110*, 4170.

(27) Wang, S.-H.; Jansen, S. A.; Singh, D. J. *J. Catal.* **1995**, *154*, 137.

(28) (a) Delley, B. *J. Chem. Phys.* **1990**, *92*, 508. (b) Delley, B. *J. Chem. Phys.* **2000**, *113*, 7756. $DMol^3$ is available as part of Materials Studio.

(29) Wang, Y.; Perdew, J. P. *Phys. Rev. B* **1991**, *44*, 13298.

(30) Delley, B. *Int. J. Quant. Chem.* **1998**, *69*, 423.

(31) Glinskaya, L. A.; Yurchenko, E. N.; Klevtsova, R. F.; Derkach, L. V.; Rios, A. M.; Lazarenko, T. P. *Zh. Strukt. Khim.* **1989**, 82.

(32) Lunk, H.-J.; Giese, S.; Fuchs, J.; Stosser, R. *Z. Anorg. Allg. Chem.* **1993**, 961.

(33) (a) Sundaram, K. M.; Neiwert, W. A.; Hill, C. L.; Weinstock, I. A. *Inorg. Chem.* **2006**, *45*, 958. (b) Neiwert, W. A.; Cowan, J. J.; Hardcastle, K. I; Hill, C. L.; Weinstock, I. A. *Inorg. Chem.* **2002**, *41*, 6950. (c) Weinstock, I. A.; Cowan, J. J.; Barbuzzi, E. M. G.; Zeng, H.; Hill, C. L. *J. Am. Chem. Soc.* **1999**, *121*, 4608.

(34) Day, V. W.; Klemperer, W. G. *Science* **1985**, *228*, 533.

(35) *Lange's Handbook of Chemistry*; Dean, J. A., Ed.; McGraw-Hill Book Co.: New York, 1985.

(36) Le Maguerès, P.; Ouahab, L.; Golhen, S.; Grandjean, D.; Peña, O.; Jegaden, J. C.; Gomez-Garcia, C. J.; Delhaès, P. *Inorg. Chem.* **1994**, *33*, 5180.

(37) Muncaster, G.; Sankar, G.; Catlow, C. R. A.; Thomas, J. M.; Coles, S. J.; Hursthouse, M. *Chem. Mater.* **2000**, *12*, 18.

(38) Casañ-Pastor, N.; Gomez-Romero, P.; Jameson, G. B.; Baker, L. C. W. *J. Am. Chem. Soc.* **1991**, *113*, 5658.

(39) Yang, Q.-H.; Zhou, D. F.; Dai, H. C.; Liu, J. F.; Xing, Y. L.; Yong, H.; Jia, H. Q. *Polyhedron* **1997**, 3985.

(40) There are three pairs of edging-sharing octahedrons $\{MO_6\}$ in the belt region of β structure but none in that of the α one.

(41) $Y = -0.048X + 3.542$ ($R = 0.98$) and $Y = -0.039X + 3.461$ ($R = 0.98$) for α and β isomers, respectively, where "*Y*" denotes the W−W distance and "*X*" denotes the absolute value of anionic charge.

(42) Considering the very small Jahn−Teller distortion of $[Co^{III}W_{12}O_{40}]^{5-}$, all the *intratriad* W−W distances (and the W−O−W angles) in the α structure are identical, and so are the *intertriad* W−W distances (and the W−O−W angles). In the *β* structure, detailed data of the two kinds of *intratriad* W−W (and W−O−W angles) and two kinds of *intertriad* W−W distances (and W−O−W angles) are provided in Tables S1 and S2 and drawn in Figure S2 in the Supporting Information.

(43) (a) Tezé, A.; Hervé, G. *J. Inorg. Nucl. Chem.* **1977**, *39*, 2151. (b) Pope, M. T. *Inorg. Chem.* **1976**, *15*, 2008. (c) Kepert, D. L. *The Early Transition Elements*; Academic Press: New York, 1972; pp 46−60, 288−304.

(44) Acerete, R.; Casañ-Pastor, N.; Bas-Serra, J.; Baker, L. C. W. *J. Am. Chem. Soc.* **1989**, *111*, 6049.

(45) Pope, M. T.; Varga, J.; Gideon, M. *Inorg. Chem.* **1966**, *5*, 1249.

(46) ΔE_{free} is the energy difference between the free relaxed $W_{12}O_{36}/C_{3v}$ and $W_{12}O_{36}/T_d$ of the *β*- and α-Keggin anions, respectively.